Appl Nanosci (2014) 4:967–978
DOI 10.1007/s13204-013-0277-y

ORIGINAL ARTICLE

Efficient adsorption of congo red dye from aqueous solution using green synthesized coinage nanoparticles coated activated carbon beads

Jolly Pal · Manas Kanti Deb

Received: 28 May 2013 / Accepted: 19 October 2013 / Published online: 13 November 2013

Abstract In this paper, the removal of congo red (CR) dye by adsorption on coinage nanoparticles [silver nanoparticles (AgNPs) and gold nanoparticles (AuNPs)] coated activated carbon (AC) has been discussed. The effect of various process parameters has been investigated by following the adsorption technique. Equilibrium adsorption data of CR were carried out at room temperature. The equilibrium time is independent of the initial CR concentration and the percentage removal of CR increased with increase in contact time. The adsorption data were analyzed by using adsorption isotherm studies. The characteristic parameters for isotherm and related correlation coefficients were determined from graphs of their linear equations. Kinetic studies showed that the adsorption of CR followed pseudo-first-order kinetics. AgNPs- and AuNPs-coated AC is found to be suitable adsorbent for the adsorption of CR. CR was effectively removed 88.0 ± 0.8 % from aqueous solution using AuNPs beads as the adsorption process. Desorption studies were made to elucidate recovery of the adsorbate and adsorbent for the economic competitiveness of the removal system. The PVP-supported AgNPs and AuNPs-coated AC were successfully recycled for ten successive adsorption–desorption cycles indicating its high reusability.

Keywords Silver nanoparticles · Gold nanoparticles · Activated carbon · Microwave irradiation · Polyvinylpyrrolidone · Congo red

J. Pal · M. K. Deb (✉)
School of Studies in Chemistry, Pandit Ravishankar Shukla University, Raipur 492 010, Chhattisgarh, India
e-mail: debmanas@yahoo.com

Introduction

Water is the most essential requirement in daily life that has been contaminated by the disposal of domestic, municipal, and industrial wastes. Anything, which is not needed, finds its way to the nearest watercourse or land, which further pollutes the ground water. So, there is a need to utilize the available resources effectively without polluting the water (Prasad and Kumar 2010). Textile industries have shown a significant increase in the use of synthetic complex organic dyes as coloring materials (Talarposhti et al. 2001). A dye is carcinogenic, affects reproductive organs and develops toxicity and neurotoxicity (Lakshmi 1987). Therefore, the dyes are to be necessarily removed from water and wastewater. Congo red (CR) is an anionic dye widely used in textiles, paper, rubber, and plastic industries. Figure 1 shows the chemical structures of CR.

Different processes for color removal typically include physical, chemical, and biological schemes. Some processes such as electrochemical techniques and ion-pair extractions are relatively new for textile waste treatment, while others have been used in the industry for a long time. Adsorption has been found to be superior to other techniques for water reuse in terms of initial cost, simplicity of design, use of operation, and insensitivity to toxic substances (Meshko et al. 2001). The lower generation of residues, easy metal recovery, and the possibility to reuse adsorbent are the greatest advantages of this method (Gurnani et al. 2003). The removal of colored and colorless organic pollutants from industrial wastewater is considered as an important application of adsorption processes (Al-Qodah 2000). The treatment of industrial effluents is a challenging topic in environmental science, as control of water pollution has become of increasing importance in

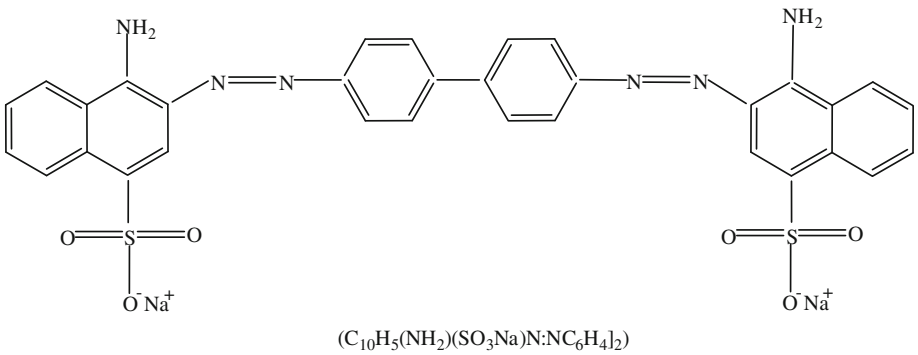

$(C_{10}H_5(NH_2)(SO_3Na)N{:}NC_6H_4]_2)$

Fig. 1 Chemical structure of CR

recent years. Phenomenologically, adsorption is generally described by a graphic representation of the distribution ratios of adsorbate adsorbed per unit mass of the adsorbent and the concentration of the unadsorbed adsorbate at constant temperature. This graphic representation is known as the adsorption isotherm. Several types of adsorption isotherm have been reported in the literature, but the most widely used are the Freundlich and Langmuir isotherms. One of the most used and successful method for the removal of organic pollutants is their adsorption on activated carbon (AC) arranged in different arrays such as filters (Sabio and Zamora 2006). AC is characterized by a high porosity and a very large surface area, which enables it to efficiently adsorb many kinds of pollutants. In spite of its high adsorption capacity, the use of AC on a large scale is limited by process engineering difficulties such as the dispersion of the AC powder and the cost of its regeneration. AC is the generic term used to describe a family of carbonaceous adsorbents with a highly crystalline form and extensively developed internal pore structure.

Metal nanoparticles (NPs) with controlled size and shape are of great interest because of their morphology-dependent properties (Schmid 1992) and potential applications in a lot of fields (Andres et al. 1996). Metal NPs have attracted considerable interest because of their novel properties and their potential application (Du et al. 2008). Binding capacity of noble metal NPs with dyes are more when compared with other NPs. Novel metal crystallites such as silver and gold provide a more interesting research field due to their close lying conduction and valence bands in which electrons move freely. The free electrons give rise to a surface plasmon absorption band, which depends on both the particle size and chemical surrounding. Right now, shape-controlled synthesis of NPs has been achieved either by using geometric templates (Zande et al. 2000), or by using some additive, such as polymers (Ahmadi et al. 1996), or inorganic anions (Filankembo et al. 2003), to regulate the particle growth. Accurate controls of size, composition, morphology and stability, and the use of environment-friendly procedures are highly desirable for the synthesis of NPs. There have been a number of techniques for NPs synthesis developed over the years using a range of metals (Pal and Deb 2012a, b, c, d, 2013; Pal et al. 2009, 2012, 2013a, b; Shah et al. 2010, 2012; Nafees et al. 2013). The most widely used substances for the stabilization of metal NPs are ligands and polymers, specially natural or synthetic polymers with a certain affinity toward metals, which are soluble in suitable solvents (Hirai et al. 1985). Such substances can also control the reduction rate of the metal ions and the aggregation process of zerovalent metal atoms. The polymers also control the aggregation of metal atoms in solution. Polyvinylpyrrolidone (PVP) is soluble in water and other polar solvents. In solution, it has excellent wetting properties and readily forms films. This makes it good as a coating or an additive to coating. PVP is used in as a binder and complexation agent in agro applications such as crop protection, seed treatment, and coating. Studies have been carried out aiming at developing more effective and selective adsorbent materials, which are abundant in nature, requiring little processing in order to decrease cost (Reddad et al. 2002). In recent years, metal NPs have attracted much research attention due to their unique electric, catalytic, and optical properties originating from the quantum-scale dimensions (Duan et al. 2005). Metal NPs have been of increasing interest in applications to biological and chemical nanosensors. One aspect of the fantastic researches on metal NPs is focused on the phenomena of aggregation or flocculation of metal NPs in solution (Liu et al. 2004). Particles aggregation results in further color changes of metal NPs solutions due to mutually induced dipoles that depend on interparticle distance and aggregate size (Lazarides and Schatz 2000). Recently, metal NPs have been applied in biosensors because of their dimensional similarities with biomacromolecules and significant size-dependent optical and electronic properties (Bukasov and Shumaker-Parry 2007). A number of attempts have been made using different experimental conditions to prepare metal NPs of different sizes and shapes.

Microwave irradiation (Rao and Ramesh 1995) is one of the novel techniques developed during the last years for the synthesis of solid materials. Microwave dielectric heating

results from dipolar polarization as a result of dipole–dipole interaction between polar molecules and electromagnetic field. It promotes the nucleation of NPs without interfering in the particle growth process. The main advantage of microwave irradiation is that it produces a uniform heating of the solution, so that a more homogeneous nucleation is obtained as well as a shorter crystallization time, when compared with conventional heating, and it is therefore very useful for the formation of monodisperse metal colloids. Further advantages are short thermal induction period, absence of convection processes, easy control, and low cost.

In this paper, green methods to synthesize silver nanoparticles (AgNPs) and gold nanoparticles (AuNPs) are described. The preparation of AgNPs and AuNPs was carried out by irradiating the solution under microwave. NPs were characterized by UV–visible spectroscopy, transmission electron microscopy (TEM), and X-ray diffraction (XRD). The adsorption behavior of CR by the PVP-supported AgNPs and AuNPs-coated AC are also given in detail in this paper. Adsorption studies were carried out to study the effects of various experimental parameters such as initial concentration, contact time, pH, and adsorbent dose were evaluated. In addition, the equilibrium isotherms, adsorption kinetics, and desorption studies of CR onto the AgNPs- and AuNPs-coated AC were also investigated.

Experimental

Materials and apparatus

$AgNO_3$ was obtained from Merck, $HAuCl_4$ was obtained from Aldrich, glucose was obtained from Molychem, PVP was obtained from Himedia and CR was obtained from LOBA. All aqueous solutions were prepared in triple-distilled water. 1×10^{-4} mol/L $AgNO_3$, 1×10^{-4} $HAuCl_4$, 0.5 mol/L glucose, 1 % PVP, and parts per million solutions of CR were used.

A Samsung CE2877 domestic microwave oven (850 W), Samsung India Electronics Ltd, New Delhi, India, was employed for irradiating solutions. The particle size and morphology of the AuNPs were characterized by Morgagni 268D transmission electron microscope operating at 80 KB (Mega view III Camera CCD) at the All India Institute of Medical Sciences (AIIMS), New Delhi. Varian Carry 50 UV–vis spectrophotometer was used for spectral studies. The XRD measurements were carried out using Bruker D8 Advance X-ray diffractometer at UGC-DAE Consortium for Scientific Research INDORE-CENTRE. The X-rays were produced using a sealed tube and the wavelength of X-ray was 0.154 nm (Cu K-alpha). The X-rays were detected using a fast counting detector based on silicon strip technology (Bruker-LynxEye detector).

Preparation of AgNPs and AuNPs

Silver nanoparticles were synthesized by using PVP as protective agent and using $AgNO_3$ as precursor and glucose as reducing agent. The reaction solution were prepared by dissolving 0.5 mol/L glucose, 1.0×10^{-4} mol/L $AgNO_3$, and 1 % PVP in triple distilled water in a 50-ml conical flask to obtain a homogeneous reaction mixture. Then the conical flask was placed on the turntable of the microwave oven. The mixture was irradiated at a power of 300 W for duration of 4 min. The reaction was carried out discontinuously to prevent an increase of pressure. After irradiation, the dilute colloidal solution with pale yellow color was cooled to room temperature and stored in a refrigerator at −4 °C for further characterization. In a similar approach, AuNPs was prepared using $HAuCl_4$ in place of $AgNO_3$. The colors of the AuNPs were purple (Pal and Deb 2012c; Pal et al. 2013b).

Fabrication of NPs

First, charcoals were locally collected, cut into small spherical shape (10 mm diameter). In order to remove the contaminants from its surface, charcoals were washed by keeping for hours the pieces into porcelain dish filled with distilled water; and after removing, dried (250 °C) on hot plate. In this process, charcoals convert to AC. Such freshly prepared AC has a clean surface. This AC produces a surface with high adsorptive capacity. Sufficient amounts of small pieces of AC were dipped into a solution of the prepared AgNPs capped with PVP, in a glass beaker (250 ml). The beaker was kept on a hot plate and the content was heated gently at 50 °C till dryness and complete removal of any moisture content. The PVP used here provides a polymeric support to fasten AgNPs over the surface of AC. The AC thus coated with AgNPs was taken for adsorption studies. In a similar approach, AuNPs-coated AC was prepared using $HAuCl_4$ in place of $AgNO_3$ (Pal and Deb 2012c; Pal et al. 2013b).

Adsorption studies

Adsorption isotherm describes the equilibrium relationship between bulk activity of adsorbate in solution and the moles adsorbed on the surface, at constant temperature. The efficiency of the removal of CR from aqueous solutions using PVP-supported AgNPs and AuNPs-coated AC was experimentally studied by recording adsorption isotherms. Adsorption experiment was conducted in which aliquots of CR solution with known concentrations were

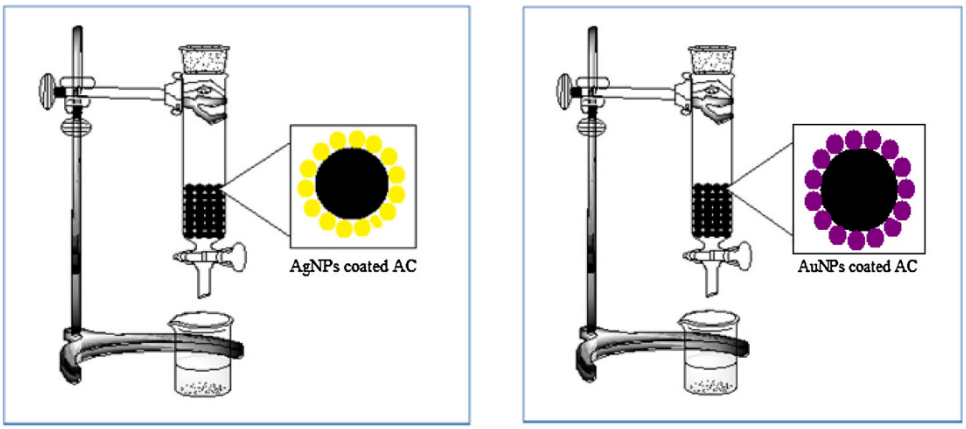

Fig. 2 Schematic diagram of column adsorption experiment

introduced into column filled with accurately weighed amount of PVP-supported AgNPs and AuNPs-coated AC. The adsorption of CR by PVP-supported AgNPs and AuNPs-coated AC was investigated in aqueous solutions at room temperature (27 °C). Figure 2 shows the schematic diagram of column adsorption experiments carried out in this work.

To determine the equilibrium adsorption capacity of the CR by PVP-supported AgNPs and AuNPs-coated AC, 100 ml of CR solution was placed separately in columns (10 cm height and 4 cm diameter) filled with accurately weighed amounts of PVP-supported AgNPs and AuNPs-coated AC. The columns, at room temperature, were sealed with stopper and left for equilibration. Aliquots of the CR solution were drained out after equilibrium time to determine the CR equilibrium concentration at a wavelength of maximum absorbance (λ_{max}), i.e., at 500 nm for CR using a UV–visible spectrophotometer.

Effects of various process parameters on the extent of removal of CR were studied. The data were analyzed statistically and interpreted. Percentage removal was calculated using the following equations:

$$\text{Percentage removal} = 100(C_i - C_e)/C_i$$

where C_i and C_e are initial and equilibrium (final) concentration of CR (mg/L), respectively. The data were analyzed statistically and interpreted. The data were modelled with Freundlich and Langmuir adsorption isotherms.

Desorption studies

Desorption of CR from PVP-supported AgNPs and AuNPs-coated AC surface were carried out as follows: after adsorption experiments with CR under optimum conditions, the PVP-supported AgNPs and AuNPs-coated AC was separated and washed with 0.05 N HNO_3 to remove adsorbed CR. The color intensity of the CR desorbed was measured UV–visible spectrophotometer. The %desorption

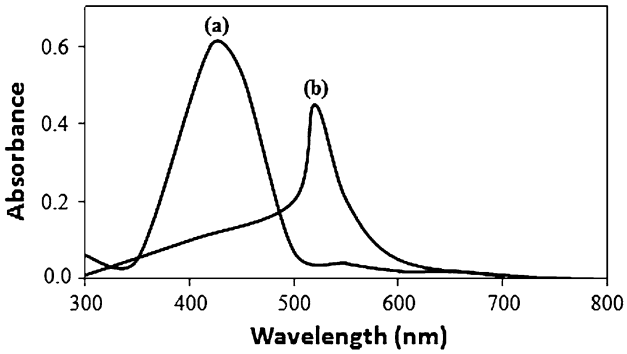

Fig. 3 UV–visible spectrum of the prepared **a** AgNPs and **b** AuNPs. Varian Carry 50 UV–visible spectrophotometer

of the CR were calculated with the help of following equation:

$$\%\text{Desorption} = \frac{\text{amount of CR liberated by acid}}{\text{amount of CR adsorbed on adsorbents}} \times 100$$

The above washed adsorbents were reused to study further the change in removal efficiency of used adsorbents.

Results and discussions

Formation of AgNPs and AuNPs

It is interesting to find that AgNPs and AuNPs can be synthesized with PVP, glucose and $AgNO_3$ for AgNPs, and $HAuCl_4$ for AuNPs promoted by microwave irradiation. Figure 3a shows the UV–visible spectrum of the prepared AgNPs in aqueous solution. The colloidal silver solution thus formed exhibits a single and strong absorption at 420 nm. The yellow color of the colloidal silver sample provides clear evidence for the formation of AgNPs. Figure 3b shows the UV–visible spectrum of the prepared

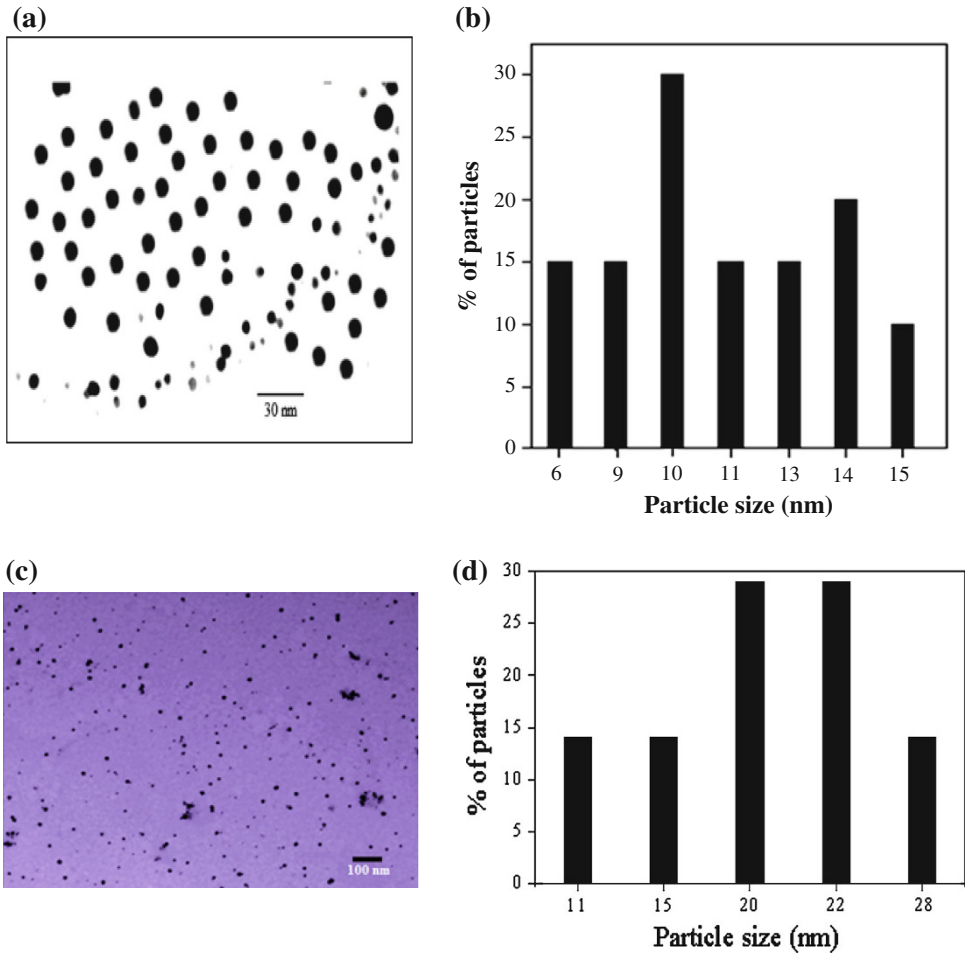

Fig. 4 **a** TEM image of the AgNPs prepared employing glucose as reducing agent and PVP as stabilizing agent (300 W; 4 min irradiation). Magnification: 13,000×; resolution: 1,376 × 1,032 × 16; image intensity: gray value; accelerating voltage: 70 kV; microscope: Morgagni 268; camera type: Keen View FW. **b** Size distributions of the AgNPs synthesized under optimum experimental conditions. **c** TEM image of the AuNPs prepared employing glucose as reducing agent and PVP as stabilizing agent (300 W; 4 min irradiation). Magnification: 25,000×; resolution: 1,376 × 1,032 × 16; image intensity: gray value; accelerating voltage: 70 kV; microscope: Morgagni 268; camera type: Keen View FW. **d** Size distributions of the AuNPs synthesized under optimum experimental conditions

AuNPs in aqueous solution. The colloidal gold solution thus formed exhibits a single peak with strong absorption at 530 nm. The purple color of the colloidal gold sample provides clear evidence for the formation of AuNPs (Pal and Deb 2012d; Pal et al. 2013b). The UV–visible spectra of the prepared AgNPs and AuNPs in aqueous solution should exhibit a single surface plasmon band, which means NPs was small and spherical (Mie 1908).

Transmission electron microscopy image was further used to characterize formed NPs. Figure 4a shows the TEM image and the corresponding particle size distribution histogram, Fig. 4b of the silver colloidal solution. The photograph shows that most of the particles are nearly spherical. The size distribution histogram reveals that such silver particles range from 6 to 15 nm in size. The 30 % of these NPs consist of particles with 10 nm diameter, 20 % particles were of 14 nm size remaining particles were in the range 6, 9, 11, 13, and 15 nm diameter sizes. The average size of AgNPs is about 11 nm via TEM images. It may be noted that all these particles are well separated from each other. AgNPs thus formed were free from flocculation or aggregation for several weeks, suggesting that the polymer serves as a very effective protective agent for AgNPs. Figure 4c shows a typical TEM image and Fig. 4d the corresponding particle size distribution histogram of AuNPs produced. The photograph shows that most of the particles are nearly spherical. The size distribution histogram reveals that such gold particles range from 11 to 28 nm in size. The 14 % of these NPs consist of particles with 11 and 15 nm diameter, 28 % particles were of 20 and 22 nm. The average size of AuNPs is about 20 nm via TEM images. It was noticed that all these particles were well separated from each other (Pal and Deb 2012d; Pal et al. 2013b).

The XRD patterns of AC- and PVP-supported AgNPs and AuNPs-coated AC, shown in Fig. 5, were also able to confirm the existence of AgNPs and AuNPs. AC shows peaks at $2\theta = 24.7°$, 29.5°, 39.5°, 43.3°, 47.4°, and 48.6°. After coating of PVP-supported AgNPs and AuNPs over AC, a significant change in XRD pattern was observed. In the PVP-supported AgNPs and AuNPs-coated AC sample new peaks appeared at $2\theta = 23.0°$, 26.6°, 29.4°, 36.0°, 39.4°, 43.2°, 47.4°, 48.4°, 57.4°, 60.6°, 64.6° and $2\theta = 23.2°$, 29.5°, 36.0°, 39.5°, 43.3°, 47.6°, 48.5°, and 57.4°, 60.6°, and 64.6°, respectively. The crystallinity of AC was apparently lower than that of the PVP-supported

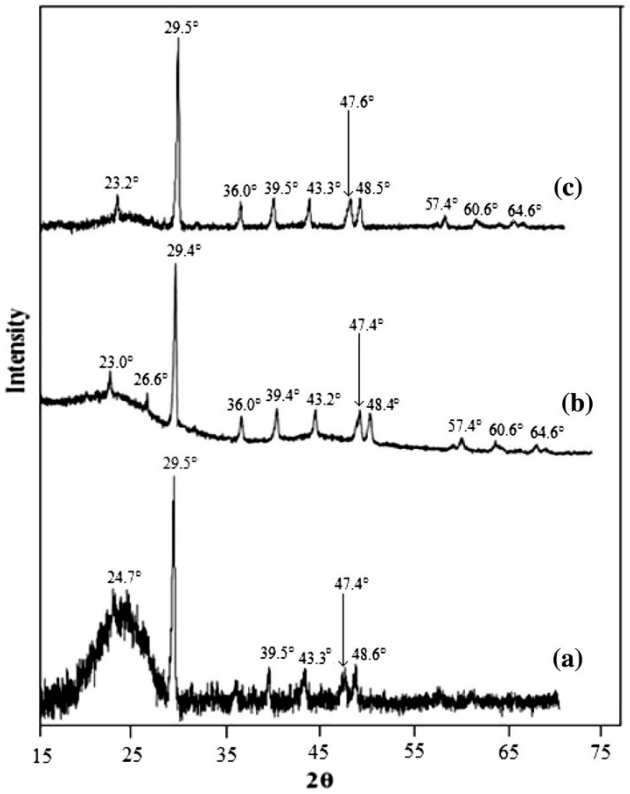

Fig. 5 XRD of **a** AC, **b** PVP-supported AgNPs-coated AC, and **c** PVP-supported AuNPs-coated AC. Bruker D8 advance X-ray diffractometer; Wavelength of S-ray was 0.154 nm (Cu K-alpha); detector based on silicon strip technology (Bruker-LynxEye detector)

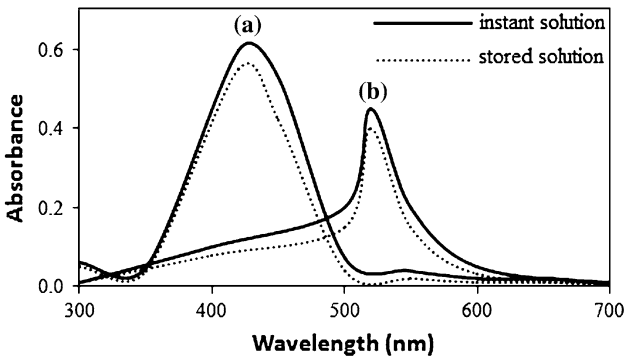

Fig. 6 UV–visible spectra of **a** AgNPs, **b** AuNPs after it is stored for 8 months in refrigerator (−4 °C)

AgNPs and AuNPs-coated AC. The results indicate that the crystallinity of PVP-supported AgNPs and AuNPs-coated AC were increased because of the formation of NPs (Pal and Deb 2012d; Pal et al. 2013b).

Effect of stabilization of AgNPs and AuNPs

As shown in Fig. 6a, b, the absorbance spectra of silver and gold colloidal solution were observed to have changed only slightly in their relative absorbance intensities, after the solution was stored for 8 months in refrigerator (−4 °C). The solution remained perfectly transparent with no obvious change in color while storage. The results implied that the AgNPs an AuNPs prepared by this method were very stable with negligible aggregation.

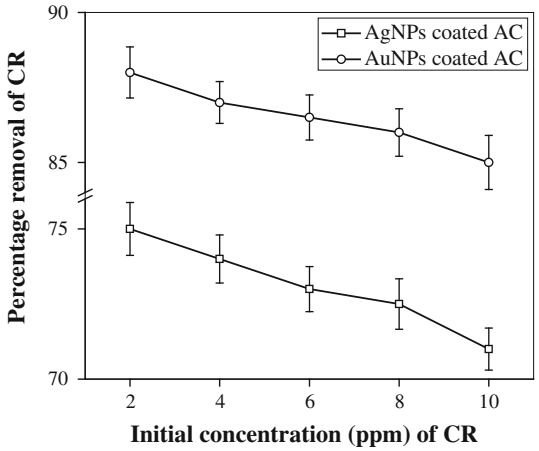

Fig. 7 Effect of initial concentration on the removal of CR by PVP-supported AgNPs and AuNPs-coated AC at room temperature ($n = 5$)

Effect of initial concentration

The effect of initial concentrations on the percentage removal of CR is shown in Fig. 7 with error bars showing the values of standard deviation ($n = 5$). The experiments were conducted at pH 6.5 ± 0.8 for CR, respectively, at room temperature. The concentrations of CR were varied from 2 to 10 mg/L. The results show that the value of percentage removal of CR decreases from 75.0 ± 0.8 to 71.0 ± 0.7 % by PVP-supported AgNPs-coated AC and 88.0 ± 0.8 to 85.0 ± 0.9 % by PVP-supported AuNPs-coated AC, respectively. Thus, the percentage removal is a direct function of initial concentrations of CR. This may probably be due to the limited number of available active sites on the surface of PVP-supported AgNPs and AuNPs-coated AC to accommodate higher concentration of CR (Li et al. 2010).

Effect of contact time

The percentage removal increased with increase in contact time and reached a constant value. This may be due to the attainment of equilibrium condition of contact time for PVP-supported AgNPs and AuNPs-coated AC. The effect of contact time on adsorption of CR with error bars showing the values of standard deviation ($n = 5$) are shown in Fig. 8. The effect of contact time was studied with initial CR concentration of 2 mg/L at pH 6.5 ± 0.8

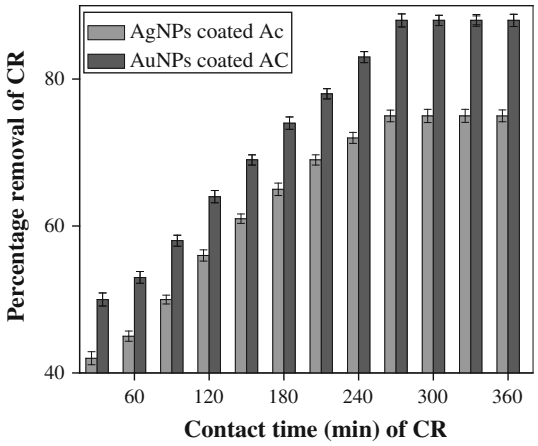

Fig. 8 Effect of contact time on the removal of CR by PVP-supported AgNPs and AuNPs-coated AC at room temperature ($n = 5$)

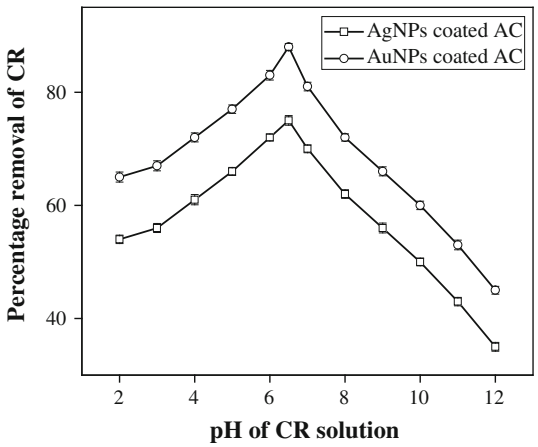

Fig. 9 Effect of pH on the removal of CR by PVP-supported AgNPs and AuNPs-coated AC at room temperature ($n = 5$)

for CR at room temperature. The percentage removal of CR for a contact time period between 30 and 270 min is 42.0 ± 0.8 to 75.0 ± 0.8 % and 50.0 ± 0.8 to 88.0 ± 0.8 % for PVP-supported AgNPs and AuNPs-coated AC, respectively.

The results show a significant improvement in percentage removal of CR by the AgNPs- and AuNPs-coated AC. At the initial stage, the rate of removal of CR was higher, due to the availability of more than required number of active sites on the surface of adsorbents and became lower at the later stages of contact time, due to the decreased or lesser number of available active sites (Kannan and Karrupasamy 1998).

Influence of pH

To study the influence of pH on the percentage removal of CR by PVP-supported AgNPs and AuNPs-coated AC, experiments were carried out at different pH values varying

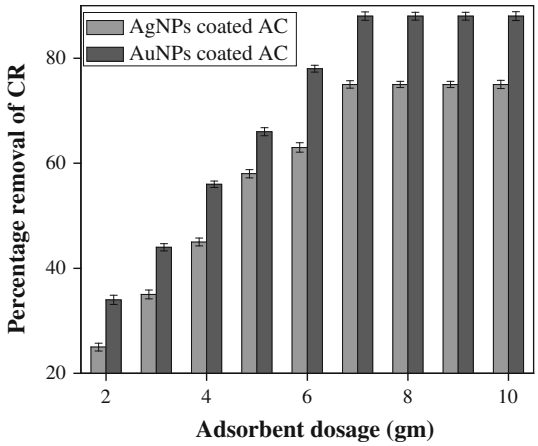

Fig. 10 Effect of adsorbent dose on the removal of CR by PVP-supported AgNPs and AuNPs-coated AC at room temperature ($n = 5$)

from 2 to 12. The observed data are presented in Fig. 9 for CR with error bars showing the values of standard deviation ($n = 5$).

It may be seen that as pH increases, the extent of removal increases, reaches to a maximum value and then decreases steadily. Therefore, the optimum pH of aqueous medium for removal of CR was fixed at 6.5 ± 0.8 for PVP-supported AgNPs and AuNPs-coated AC adsorbent systems.

Effect of adsorbent dosage

Adsorbent dose is an important parameter in the determination of adsorption capacity. The effect of the adsorbent dose was investigated by the addition of various amounts of adsorbent from 2 to 10 g in 100 mL aqueous solution of CR (2 mg/L) at room temperature for equilibrium time. The result is shown in Fig. 10. It is evident from the plots that the percentage removal of CR from the aqueous solution increases with increase in the adsorbent dosage.

It was observed that the removal efficiency increased from 25 ± 0.8 to 75 ± 0.8 % and 34.0 ± 0.8 to 88.0 ± 0.8 % for CR with the adsorbent dose varying from 2 to 7 g of PVP-supported AgNPs and AuNPs-coated AC, respectively, and there after reached a constant value. It is readily understood that the number of available adsorption sites increases by increasing the adsorbent dose and it therefore results in an increase in the percentage of CR adsorbed.

Adsorption isotherm

The adsorption characteristics for wide range of adsorbate concentrations are mostly described by adsorption isotherm (Freundlich and Langmuir), which relates the equilibrium adsorbate concentration in the bulk and the uptake of

adsorbate on the adsorbent surface. Freundlich isotherm is presented by the following relation:

$$\ln Q_e = \ln K_F + \ln C_e$$

where K_F and n are Freundlich constant, a characteristic of the system indicating the adsorption capacity (mg/g), and adsorption intensity or surface heterogeneity, respectively.

The Langmuir isotherm is valid for monolayer adsorption onto a surface containing a finite number of identical sites.

$$\frac{C_e}{Q_e} = \frac{b}{Q_0} + \frac{C_e}{Q_0}$$

where C_e is the equilibrium dye concentration in the solution (mg/L), Q_e is the equilibrium dye concentration on the adsorbent (mg/g), Q_0 is the maximum adsorption capacity of the dye (forming a monolayer) per unit weight of adsorbent (mg/g), and b is a constant related to the affinity of the binding sites (L/mg).

The essential characteristics of the Langmuir isotherm can be expressed by a separation factor R_L (Mall et al. 2005), which is defined in the following equation:

$$R_L = \frac{1}{1 + bC_0}$$

The R_L value shows the nature of the adsorption process to be unfavorable ($R_L > 1$), linear ($R_L = 1$), favorable ($0 < R_L < 1$), or irreversible ($R_L = 0$).

The adsorption isotherm of CR was investigated at optimized condition pH 6.5 ± 0.8 at room temperature. As seen from the Fig. 11a, the Freundlich model described the equilibrium adsorption process. The values for CR on the Freundlich parameters n and K_F were 1.12, 24.82 ± 0.45 mg/g for PVP-supported AgNPs-coated AC; and 1.14, 28.40 ± 0.55 mg/g for PVP-supported AuNPs-coated AC, respectively. Figure 11b present the Langmuir plots for the adsorption of CR onto PVP-supported AgNPs and AuNPs-coated AC. The values for CR on the Langmuir parameters Q_0 and b were 0.47 ± 0.45 mg/g, 0.09 L/mg for PVP-supported AgNPs-coated AC; and 0.50 ± 0.55 mg/g, 0.22 L/mg for PVP-supported AuNPs-coated AC, respectively. The results obtained from adsorption isotherms, according to Freundlich and Langmuir models are shown in Table 1. Freundlich values indicated high adsorption capacity of CR on PVP-supported AgNPs and AuNPs-coated AC when compared to the Langmuir isotherm model, in which adsorption is based on heterogeneous surface of adsorbents and Freundlich isotherm is not restricted to the formation of the monolayer (Mohammadi et al. 2011). The adsorption capacity was much faster when PVP-supported AuNPs-coated AC was the adsorbent as compared with PVP-supported AgNPs-coated AC. It is estimated from the adsorption experiment that loading in the case of PVP-supported AuNPs-coated AC is much more compared to PVP-supported AgNPs-coated AC (Saha et al. 2009).

Adsorption kinetics

The percentage removal of CR at a fixed adsorbent dose (7 g) was monitored at different time intervals. The kinetics of CR removal by PVP-supported AgNPs and AuNPs-coated AC indicated rapid binding of CR to the PVP-supported AgNPs and AuNPs-coated AC during first few minutes, followed by a slow increase until a state of equilibrium time was reached. No change in the uptake capacity was observed with further increase in equilibrium time. The initial rapid phase may be due to increased number of vacant sites available at the initial stage. Generally, when adsorption involves a surface reaction process, the initial adsorption is rapid. Then, a slower adsorption would follow as the available adsorption site gradually decreases (Kannan and Karrupasamy 1998).

The adsorption kinetics can be described by the pseudo-first-order kinetic model and the pseudo-second-order kinetic model (Eftekhari et al. 2010; Dogan et al. 2007). The pseudo-first-order equation is generally expressed as following:

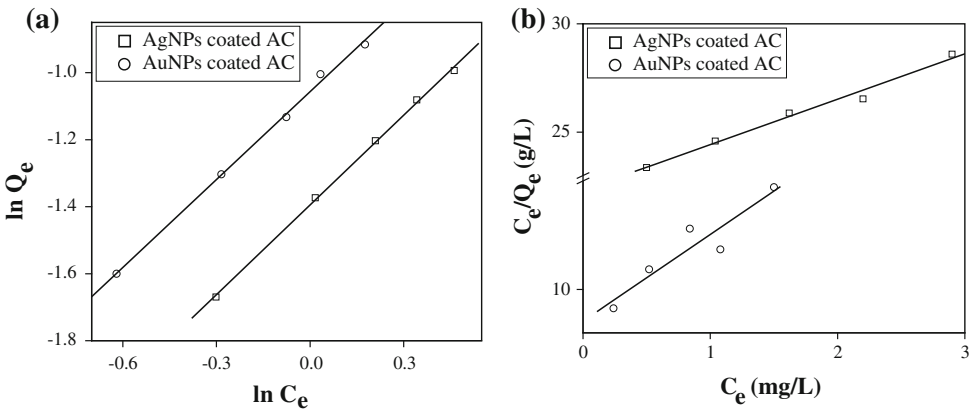

Fig. 11 **a** Freundlich isotherm. **b** Langmuir isotherm plot for adsorption of CR on PVP-supported AgNPs and AuNPs-coated AC at room temperature

$$\left(\frac{1}{q_t}\right) = \left(\frac{k_1}{q_e}\right)\left(\frac{1}{t}\right) + \left(\frac{1}{q_e}\right)$$

Kinetics of adsorption was modelled by the pseudo-second-order equation as shown below.

$$\frac{t}{q_t} = \frac{t}{q_e} + \frac{1}{q_e^2 k_2}$$

where, q_e and q_t are the equilibrium adsorption capacity (mg/g) and the adsorption capacity at time t, respectively; k_1 is the rate constant of pseudo-first-order adsorption (time^{-1}). The plot of q_t versus t should give a linear relationship from which k_1 and q_e can be determined from the slope and intercept of the plot, respectively. Here, k_2 is the pseudo-second-order rate constant of adsorption (g/mg/time). The plot is a linear relationship between t/q_t and t, q_e and k_2 can be determined from the slope and intercept of the plot of t/q_t versus t, respectively. Graphical representation of pseudo-first-order equation is shown in Fig. 12a for CR when adsorbed onto PVP-supported AgNPs and AuNPs-coated AC. Graphical representation of pseudo-second-order equation is shown in Fig. 12b for CR when adsorbed onto PVP-supported AgNPs and AuNPs-coated AC. The correlation coefficients (R^2), adsorption capacity (q_e), and the rate constant for adsorbents are summarized in Table 2. For all the systems studied, good correlation coefficients were obtained by fitting the experimental data to pseudo-first-order and pseudo-second-order kinetics. The adsorption kinetic data, however, fitted best in pseudo-first-order model, where linear plot of t versus q_t was obtained. Pseudo-first-order values indicated that the adsorption of CR on PVP-supported AgNPs and AuNPs-coated AC were high adsorption capacity and correlation coefficients than pseudo-second-order, which can be ascribed to the effective physical adsorption of CR onto adsorbents.

Table 1 Adsorption isotherm data for removal of CR by PVP-supported AgNPs and AuNPs-coated AC at room temperature

Adsorbent	Freundlich constants			Langmuir constants			
	K_F (mg/g)	n	R^2	Q_0 (mg/g)	b (L/mg)	R^2	R_L
AgNPs-coated AC	24.82 ± 0.45	1.12	0.99	0.47 ± 0.45	0.09	0.99	0.84
AuNPs-coated AC	28.40 ± 0.55	1.14	0.99	0.50 ± 0.55	0.22	0.88	0.70

Desorption studies

Desorption studies help to elucidate the nature of adsorption and to the recovery of the valuable adsorbate and adsorbent. To make the adsorbent economically competitive, the prepared composite materials should be reused for 'n' number of cycles.

Attempts were made to the effective desorption of CR from the spent PVP-supported AgNPs and AuNPs-coated AC using 0.05 N HNO_3. Percentage removal of CR by PVP-supported AgNPs and AuNPs-coated AC is shown in Fig. 13.

It was observed that the percentage removal of PVP-supported AgNPs and AuNPs-coated AC was almost same after ten adsorption–desorption cycles. This result shows that PVP-supported AgNPs and AuNPs-coated AC is good reusable adsorbent for the removal of CR from aqueous solution.

Comparison with other studies

Table 3 shows a list of adsorbents used in wastewater treatment for CR. Because of its great capacity to remove CR, AC is the most effective adsorbents. The loss of AC during recycling process by HNO_3 was prevented by the coating of NPs over it. Additionally, NPs provide more surface area for adsorption to occur on it and consequently this enhances the adsorption efficiency. Table 4 shows the extent of removal of the tested CR by different adsorbents at the optimized condition. It is clear from the observed data that the maximum degree of adsorption for different

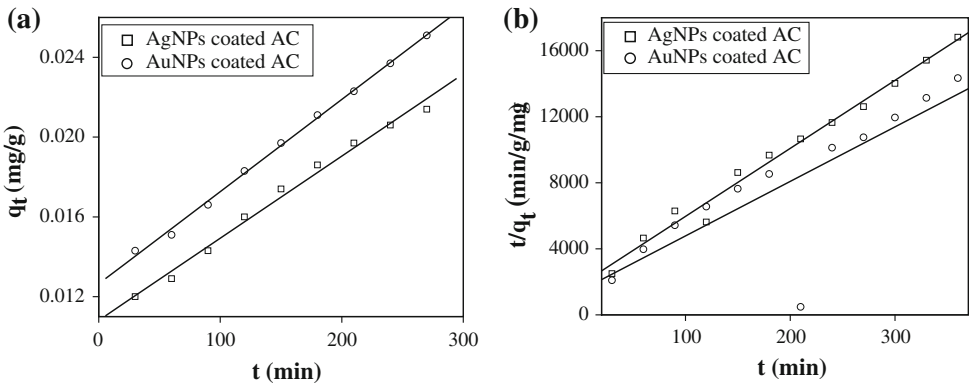

Fig. 12 **a** Pseudo-first-order and **b** pseudo-second-order kinetic plot for the removal of CR by PVP-supported AgNPs and AuNPs-coated AC

Table 2 Adsorbents value calculated using the pseudo-first-order and pseudo-second-order kinetic models for the CR at room temperature

S. no.	Adsorbent	Pseudo-first-order			Pseudo-second-order		
		q_e (mg/g)	k_1 (h^{-1})	R^2	q_e (mg/g)	k_2 (g/mg/h)	R^2
1.	AgNPs-coated AC	79.36 ± 0.45	0.039	0.998	0.025 ± 0.451	0.73	0.991
2.	AuNPs-coated AC	92.59 ± 0.55	0.037	0.990	0.029 ± 0.552	0.57	0.986

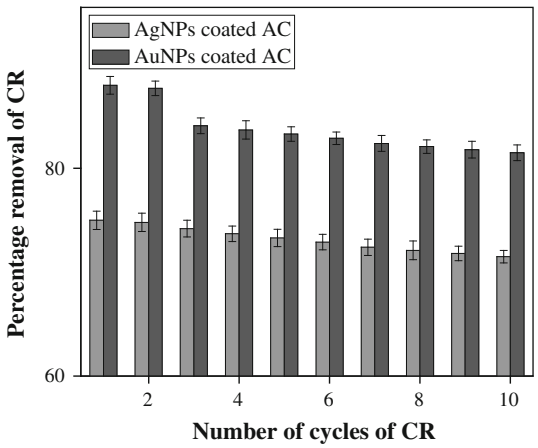

Fig. 13 Percentage removal of CR by PVP-supported AgNPs and AuNPs-coated AC after adsorption–desorption cycles ($n = 5$)

adsorbent systems, at a minimum concentration of CR tested, is in the order AC-PVP-AuNPs > AC-PVP-AgNPs > AC-PVP > AC.

Conclusion

Silver nanoparticles and AuNPs have been synthesized rapidly in chemically green condition. AgNPs and AuNPs were synthesized from $AgNO_3$ and $HAuCl_4$, respectively, using glucose as reducing agent and PVP as stabilizing agent. The particles were characterized by UV–visible spectroscopy, TEM, and XRD analysis and they were found to be spherical and crystalline and with average size of 11 nm AgNPs and 20 nm AuNPs. The investigation on the formation of AgNPs and AuNPs using UV–visible spectroscopy has shown that the AgNPs and AuNPs formed are nanosized, uniformly distributed and absorption peak at 420 for AgNPs and at 530 nm for AuNPs. In this work, the newly synthesized adsorbent, i.e., AC modified with NPs was applied successfully for separation of CR. The experiments were performed with CR initial concentrations varying from 2 to 10 mg/L. The percentage removal increases with increase in contact time. The adsorption equilibrium was reached at about 270 min for CR. The pH 6.5 ± 0.8 for CR were found most favorable and at this pH the percentage removal is high at room temperature (27 °C). The data are well represented by Freundlich isotherm and Langmuir isotherm indicating favorable adsorption of CR by the PVP-supported AgNPs and AuNPs-coated AC. The characteristic parameters for isotherm and related correlation coefficients were determined from graphs of their linear equations. The maximum adsorption capacity from Freundlich isotherm model were 24.82 ± 0.45 mg/g for PVP-supported AgNPs-coated AC and 28.40 ± 0.55 mg/g for PVP-supported AuNPs-coated AC of CR. This indicates the adsorption is based on heterogeneous surface of adsorbents and Freundlich isotherm is not restricted to the formation of the monolayer. The data on kinetic studies indicated that the adsorption kinetics of CR on PVP-supported AgNPs and AuNPs-coated AC followed the pseudo-first-order and pseudo-second-order model at room temperature. The data on kinetic studies indicated that the adsorption kinetics of CR on PVP-supported AgNPs and AuNPs-coated AC followed the pseudo-

Table 3 Recent reported adsorbent systems for CR

S. no.	Adsorbents	Adsorption capacities (mg/g)	Percentage removal (%)	Economic viability	Sources
1	Rice husk carbon activated by steam	–	99	–	Sharma and Janveja, 2008
2	Anilinepropylsilica xerogel	22.62	97	–	Pavan et al., 2008
3	Hydrogen peroxide treated tendu waste	134.4	73	–	Nagda and Ghole, 2009
4	AgNPs-coated AC	64.80	75	Percentage removal almost same after 10 cycles	Present work
5	AuNPs-coated AC	71.05	88	Percentage removal almost same after 10 cycles	Present work

Table 4 Removal of CR by different adsorbents at optimized condition (pH ~6.5, 27 °C, 270 min)

S. no.	Dye (mg/L)	AC (%)	PVP-supported AgNPs-coated AC (%)	PVP-supported AuNPs-coated AC (%)	PVP-supported AC (%)
1.	2.0	53.0	75.0	88.0	63.0
2.	4.0	50.3	74.0	87.0	60.0
3.	6.0	48.5	73.0	86.0	59.3
4.	8.0	47.0	72.5	86.5	57.6
5.	10	46.2	71.0	85.0	56.1

first-order kinetics indicating physicosorptions. The regeneration of PVP-supported AgNPs and AuNPs-coated AC is found almost same even after at least ten cycles. Adsorption capacity of PVP-supported AuNPs-coated AC seems to be superior than the PVP-supported AgNPs-coated AC for CR because the loading of PVP-supported AuNPs-coated AC is much high when compared with PVP-supported AgNPs-coated AC in adsorption experiments.

References

Ahmadi TS, Wang ZL, Green TC, Henglein A, El-Sayed MA (1996) Shape-controlled synthesis of colloidal platinum nanoparticles. Science 272:1924–1926

Al-Qodah Z (2000) Adsorption of dyes using shale oil ash. Water Res 34:4295–4303

Andres RP, Bielefeld JD, Henderson JI, Janes DB, Kolagunta VR, Kubiak CP, Mahoney WJ, Osifchin RG (1996) Self-assembly of two-dimensional superlattice of molecularly linked metal clusters. Science 273:1690–1693

Bukasov R, Shumaker-Parry JS (2007) Highly tunable infrared extinction properties of gold nanocrescents. Nano Lett 7:1113–1118

Dogan M, Ozdemir Y, Alkan M (2007) Adsorption kinetics and mechanism of cationic methyl violet and methylene blue dyes onto sepiolite. Dyes Pigm 75:701–713

Du BD, Phu DV, Duy NN, Lan NTK, Lang VTK, Thanh NVK, Phong NTP, Hien NQ (2008) Preparation of colloidal silver nanoparticles in ploy (*N*-vinylpyrrolidone) by γ-irradiation. J Exp Nanosci 3(3):207–213

Duan HY, Chen F, Ai XP, He ZK (2005) The interaction between propranolol and gold nanoparticles and its analytical application. Chin Chem Lett 16:947–950

Eftekhari A, Yangjeh H, Sohrabnezhad S (2010) Application of AIMCM-41 for competitive adsorption of methylene blue and rhodamine B: thermodynamic and kinetic studies. J Hazard Mater 178:349–355

Filankembo A, Giorgio S, Lisiecki I, Pileni MP (2003) Is the anion the major parameter in the shape control of nanocrystals. J Phys Chem B 107:7492–7500

Gurnani V, Singh AK, Venkataramani B (2003) Cellulose functionalized with 8-hydroxyquinoline: new method of synthesis and applications as a solid phase extractant in the determination of metal ions by flame atomic absorption spectrometry. Anal Chim Acta 485:221–232

Hirai H, Chawanya H, Toshima N (1985) Synthesis and properties of a chelating resin containing a macrocyclictetraaza system as active group. React Polym 3:127–135

Kannan N, Karrupasamy K (1998) Low cost adsorbents for the removal of phenyl acetic acid from aqueous solution. Indian J Environ Prot 18:683–690

Lakshmi D (1987) Influence of the dyestuff effluents of a textile processing unit, Cauvery river, erode on the activity and glycogen content of brain, liver, heart and muscle tissue. M. Phil. Dissertation. Bharathiar University, Coimbatore

Lazarides AA, Schatz GC (2000) DNA-linked metal nanosphere materials: structural basis for the optical properties. J Phys Chem B 104:460–467

Li G, Du Y, Tao Y, Deng H, Luo X, Yang J (2010) Iron (II) cross-linked chitin-based gel beads: preparation, magnetic property and adsorption of methyl orange. Carbohydr Polym 82:706–713

Liu XL, Yuan H, Pang DW (2004) Resonance light scattering spectroscopy study of interaction between gold colloid and thiamazole and its analytical application. Spectrochim Acta A 60:385–389

Mall ID, Srivastava VC, Agarwal NK, Mishra IM (2005) Removal of congo red from aqueous solution by bagasse fly ash and activated carbon: kinetic study and equilibrium isotherm analyses. Chemosphere 61:492–501

Meshko V, Markovska L, Minchev M, Rodrigues AE (2001) Adsorption of basic dyes on granular activated carbon and natural zeolite. Water Res 35:3357–3366

Mie G (1908) Beitrage zur Optik truber Medien, speziell kolloidaler Metallosungen. Ann Phys 25:377–445

Mohammadi N, Khani H, Gupta VK, Amereh E, Agarwal S (2011) Adsorption process of methyl orange dye onto mesoporous carbon material—kinetic and thermodynamic studies. J Colloid Interface Sci 362:457–462

Nafees M, Ali S, Idrees S, Rashid K, Shafique M (2013) A simple microwave assists aqueous route to synthesis CuS nanoparticles and further aggregation to spherical shape. Appl Nanosci 3:119–124

Nagda GK, Ghole VS (2009) Biosorption of congo red by hydrogen peroxide treated tendu waste. Iran J Environ Health Sci Eng 6:195–200

Pal J, Deb MK (2012a) Effective removal of brilliant green dye from aqueous solution by adsorption onto biopolymer supported silver nanoparticles beads. J Indian Chem Soc 89:1689–1695

Pal J, Deb MK (2012b) Green formation and catalytic activity of palladium nanoparticles on brilliant green in aqueous solution. Indian J Environ Prot 32:574–578

Pal J, Deb MK (2012c) Microwave green synthesis of PVP stabilized gold nanoparticles and their adsorption behaviour for methyl orange. J Exp Nanosci. doi:10.1080/17458080.2012.667160

Pal J, Deb MK (2012d) Microwave synthesis of polymer coated silver nanoparticles by glucose as reducing agent. Indian J Chem Sec A 51:821–824

Pal J, Deb MK (2013) Efficient sorption of basic organic dyes from aqueous solution using green synthesized silver nanoparticles beads. J Dispers Sci Technol 34:1193–1201

Pal A, Shah S, Devi S (2009) Microwave-assisted synthesis of silver nanoparticles using ethanol as a reducing agent. Mater Chem Phys 114:530–532

Pal J, Deb MK, Deshmukh DK, Sen BK (2012) Microwave-assisted synthesis of platinum nanoparticles and their catalytic degradation of methyl violet in aqueous solution. Appl Nanosci. doi:10.1007/s13204-012-0170-0

Pal J, Deb MK, Deshmukh DK (2013a) Microwave-assisted synthesis of silver nanoparticles using benzo-18-crown-6 as reducing and stabilizing agent. Appl Nanosci. doi:10.1007/s13204-013-0229-6

Pal J, Deb MK, Deshmukh DK, Verma D (2013b) Removal of methyl orange by activated carbon modified by silver nanoparticles. Appl Water Sci 3:367–374

Pavan FA, Dias SLP, Lima EC, Benvenutti EV (2008) Removal of congo red from aqueous solution by anilinepropylsilica xerogel. Dyes and Pigm 76:64–69

Prasad A, Kumar P (2010) Biosortion of cadmium: equilibrium, kinetics and thermodynamics by *Erythrina variegata* orientalis leaf powder. Intern J Chem Eng Res 2:173–180

Rao KJ, Ramesh PD (1995) Use of microwaves for the synthesis and processing of materials. Bull Mater Sci 18:447–465

Reddad Z, Gerente C, Andres Y, Cloirec P (2002) Adsorption of several metal ions onto a low cost biosorbent: kinetic and equilibrium studies. Environ Sci Technol 36:2067–2073

Sabio E, Zamora F (2006) Adsorption of p-nitrophenol on activated carbon fixed-bed. Water Res 40:3053–3060

Saha S, Pal A, Pande S, Sarkar S, Panigrahi S, Pal T (2009) Alginate gel-mediated photochemical growth of mono- and bimetallic gold and silver nanoclusters and their application to surface-enhanced Raman scattering. J Phys Chem C 113(18):7553–7560

Schmid G (1992) Large clusters and colloids—metals in the embryonic state. Chem Rev 92:1709–1727

Shah S, Pal A, Gude R, Devi S (2010) Synthesis and characterization of thermo responsive copolymeric nanoparticles of poly (methyl methyacrylate-co-*N*-vinylcaprolactam. Eur Polym J 46(5):958–967

Shah B, Tailor R, Shah A (2012) Equilibrium, kinetics, and breakthrough curve of phenol sorption on zeolitic material derived from BFA. J Dispers Sci Technol 33:41–51

Sharma J, Janveja B (2008) A study on removal of congo red dye from the effluents of textile industry using rice husk carbon activated by steam. Rasayan J Chem 4:936–942

Talarposhti AM, Donnelly T, Anderson GK (2001) Colour removal from a simulated dye wastewater using a two-phase anaerobic packed bed reactor. Water Res 35:425–432

Zande BMI, Bohmer MR, Fokkink LGJ, Sehonenberger C (2000) Colloidal dispersions of gold rods: synthesis and optical properties. Langmuir 16:451–458